(B) Multipole pairing vibrations: (405)a

Although much work has been carried out concerning multipole pairing vibrations,*) i.e. modes with transfer quantum numbers $\beta = \pm 2$ and multipolarity and parity λ^π different from 0^+, this remains a chapter essentially missing from the subject of pairing in nuclei. Arguably with the partial exception of quadrupole pairing, studied in the multiphonon pairing vibrational spectrum around the closed shell ^{208}Pb, and in connection with strongly excited 0^+ pairing vibrational states in the actinide region **)

In what follows, we shall elaborate on the new insight on pairing vibrational modes, the studies of two-neutron pickup reactions on ^{11}Li have opened. As already explained, because (A)-(A) pp 19-22 Phys. Scripta.

to p. 405

(B)

to p. 405

*) See Bromley, D. and Broglia (2005) Sect. 5.3 and refs therein.

**) It is of notice that β-vibrations and monopole pairing vibrations strongly mix in quadrupole deformed nuclei.

of states. Also of those problems arising from the identity of the particles appearing explicitly and those participating in the collective modes (Pauli principle). NFT thus provides the theoretical framework to obtain an accurate microscopic solution of the many-body nuclear problem. Because of the validity of these solutions concerning both bound and continuum states, the NFT rules allow for a unified treatment of both structure and reactions. The program concerning reactions is lively under way, the calculation of the polarization contribution to the optical potential constituting one of the important challenges.

Summing up, the implementation of NFT rules allows for a correct and unified description of nuclear structure and reactions. In a very real sense this (NFT diagrams shown in e.g. figures 2 and 12, and eventually those describing anelastic processes) is a nucleus. Namely, the summed information (figures 1–3 and 12 (^{11}Li) ; table 1 and figures 6 and 8 (^{120}Sn)), carried to the detectors by asymptotic states, of the outcome of probing the system with a complete array of experiments (elastic, anelastic, one- and two-nucleon transfer processes).

This is unarguably what NFT can do, as testified by the documentation presented here or referred to. What it cannot do, is to solve problems regarding ill behaved bare forces, or the consequences of associated PVC vertices which eventually lead to divergences. Within this context, empirical renormalization has proven to be a powerful and physically consistent prescription to implement the NFT program and make connection with experimental data.

7. Hindsight

As a result of the ground breaking contributions of Bohr and Mottelson which we celebrate in the present volume, our understanding of the nuclear structure is based on independent particle and collective elementary modes of excitations and of their couplings. The NFT program uses these modes and couplings to consistently build a many-body effective field theory (see e.g. figure 7), removing spurious Pauli principle violating terms and non-orthogonality contributions (see e.g. figure 4). It is possible then to utilize the resulting many-body correlated wavefunctions for the description of the nuclear structure observables (see e.g. figure 1) and nuclear reaction cross sections (see e.g. figures 3 and 8). The program, although rather well implemented, is not yet fully operative (in particular concerning its reaction part). Not only for the intrinsic difficulties in developing such a complete description of the many-body nuclear structure and reactions phenomena in itself, but also due to inconsistencies in mean field generators leading to uncontrollable spuriosities which only now are being addressed.

To overcome such and others, external, present-day limitations to the validity of the NFT treatment of the nuclear many-body problem, we implemented an empirical renormalization procedure: tune the PVC vertex to reproduce the experimental properties of low-lying collective states with separable interactions making use of experimental single-particle levels, and treat this procedure as an ansatz which has to consistently recover itself in the RPA calculation of the collective states.

To quote but just two results and one outstanding open problem of the implementation of the NFT program:

(a) The pairing gap of spherical open-shell nuclei is made of essentially *equal contributions* arising from the bare NN–$^1S_0$ and from the induced pairing interactions. That is from short and from long range interactions.

(b) Making use of NFT wavefunctions and associated spectroscopic amplitudes, *one can calculate* two-nucleon transfer absolute differential cross sections which provide an overall account of the observations within experimental errors.

(c) Making use of NFT wavefunctions and associated spectroscopic amplitudes, *calculate* the polarization contribution to the nucleon–nucleus optical potential in general, and to that describing the elastic scattering of a proton off ^{11}Li in particular.

Appendix A. Neutron halo pair addition mode and GDPR: symbiotic elementary mode of nuclear excitation

Halo states like $|^{11}\mathrm{Li(gs)}\rangle$, in which a consistent fraction of the two weakly bound neutrons forms an extended low density misty cloud, imply the presence of a low-lying dipole state. It results from the sloshing back and forth of the neutron cloud involving also those of the core, with respect to the protons of the core. Microscopically, to form a halo, the two neutrons have to move in weakly bound or virtual single-particle states, with no or little centrifugal barrier. That is, s- and p-states strongly renormalized, and as a result, both lying essentially at threshold. Thus the presence of low-energy $(s, p)_{1^-}$ configuration which, coupling to the giant dipole resonance can bring down a fraction of the dipole (TRK) sum rule.

Because of the small overlap existing between halo neutrons and core nucleons both the $^1S_0$, NN- and the symmetry-potential become strongly screened, resulting in a subcritical value of pairing strength and in a weak repulsion to separate protons from neutrons in the dipole channel. As a result, neither the $J^\pi = 0^+$ correlated neutron state (Cooper pair), nor the $J = 1^-$ one (vortex-like) are bound (although both qualify[37] to do so) to the core ^{9}Li.

Having essentially exhausted the bare NN-interaction channels, the two neutrons can correlate their motion by exchanging vibrations of the medium in which they propagate, namely the halo and the core. Concerning the first one, these modes could hardly be the $\lambda = 2^+$, 3^- or 5^- surface vibrations found in nuclei lying along the stability valley. This is because the diffusivity of the halo is so large that it blurs the very definition of surface. Those associated with the core (2^+ see figure A1 (c), 3^-, 5^- etc) provide some glue, but insufficient to bind any of the two dineutron states in question.

The next alternative is that of bootstrapping. Namely, that in which the two partners of the (monopole) Cooper pair exchange pairs of vortices (dipole Cooper pair), as well as one dipole Cooper pair and a quadrupole pair removal mode, while those of the vortex exchange pairs of Cooper pairs (monopole

[37] Within this context note the detailed dependence on quantal size effects of these 'exotic nuclei' excitations as compared to those discussed in [160].

as already mentioned, the

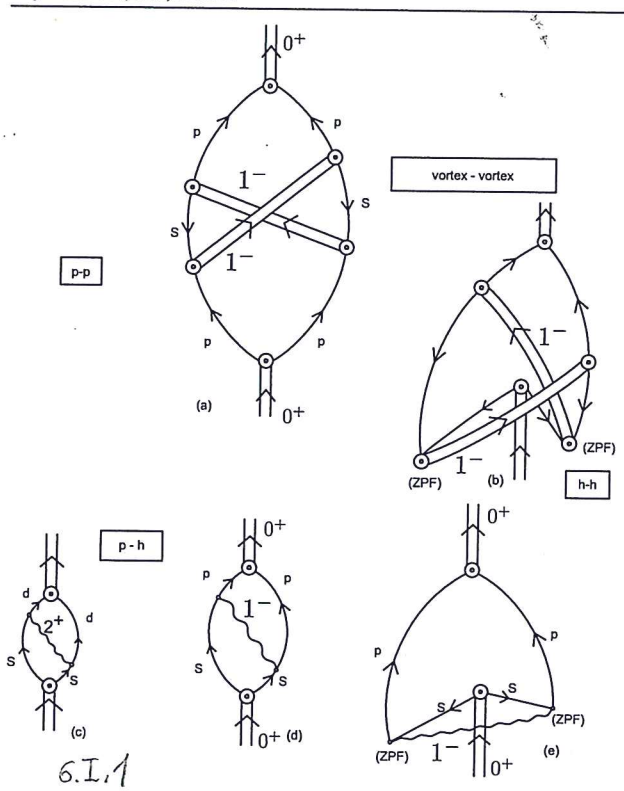

Figure A1. NFT-Feynman diagrams describing the interweaving between the neutron halo pair addition monopole and dipole modes (double arrowed lines labeled 0^+ and 1^- respectively). Above, the exchange of dipole modes binding the 0^+ pair addition mode through forwards going particle–particle p–p (h–h) components. Below, the assumption is made that the GDPR of ^{11}Li can be viewed as a p–h (two quasiparticle), QRPA mode.

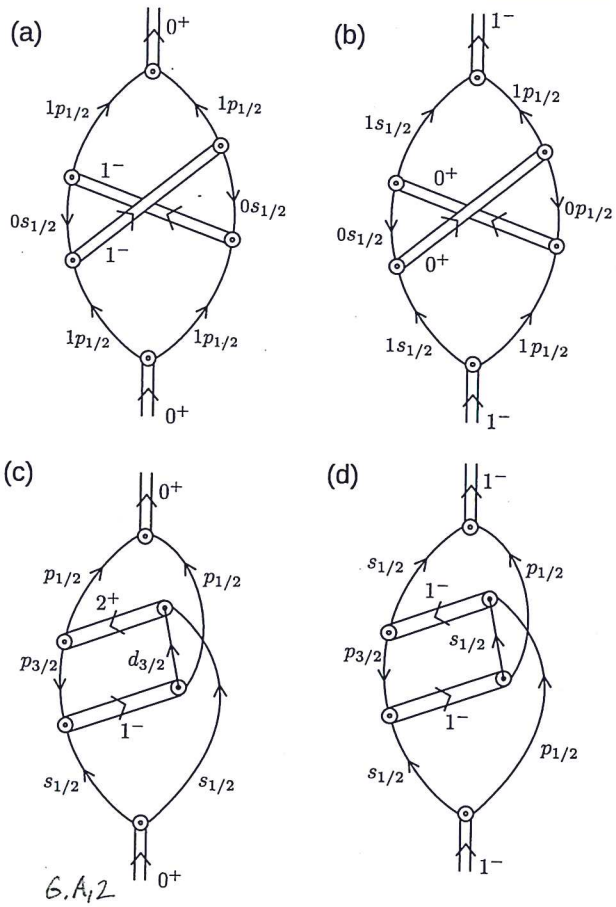

Figure A2. NFT-Feynman diagrams describing, (a) and (c) some of the particle-particle (pp), hh and ph processes binding the Cooper pair neutron halo and stabilizing ^{11}Li, as well as (b) and (d) giving rise to the GDPR.

pairing vibrations), but also pairs of dipole pairs, as shown in figures A1 and A2. In other words, by liaising with each other, the two dineutrons contenders at the role of ^{11}Li ground state settle the issue. As a result the Cooper pair becomes weakly bound (S_{2n} = 389 keV), the vortex state remaining barely unbound, by about 0.5–1 MeV [71, 72]. There is no physical reason why things could not have gone the other way, at least none that we know. Within this context we refer to ^{3}He superfluidity, where condensation involve $S = 1$ pairs. It is of notice that we are not considering spin degrees of freedom in the present case, at least not dynamic ones.

For practical purposes, one can describe the 1^- as a two quasiparticle state and calculate it within the framework of QRPA adjusting the strength of the dipole–dipole separable interaction to reproduce the experimental findings [67]. In this basis it is referred to as a GDPR. Exchanged between the two partners of the Cooper pair (figure A1(d)) leads to essentially the right value of dineutron binding to the ^{9}Li core. Within this context one can view the ^{11}Li neutron halo as a van der Waals Cooper pair (figure A1(e)). The transformation between this picture and that discussed in connection with (a) and (b) as well as with figure A2 can be obtained expressing the GDPR, QRPA wavefunction, in terms of particle creation and destruction operators (Bogoliubov–Valatin transformation) as seen from figures A1(a) and (b). A vortex–vortex stabilized Cooper pair emerges.

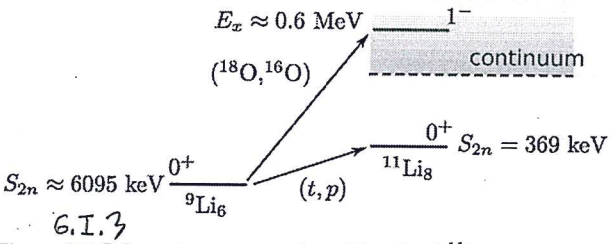

Figure A3. Schematic representation of levels of ^{11}Li populated in two-nucleon transfer reactions. Indicated in keV are the two-neutron separation energies S_{2n}. In labelling the different states, one has not considered the quantum numbers of the $p_{3/2}$ odd proton.

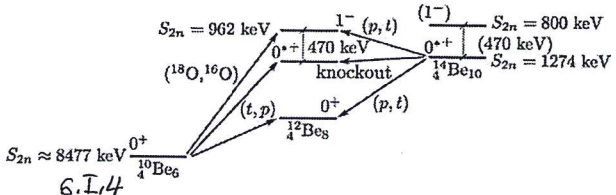

Figure A4. Levels of ^{12}Be expected to be populated in two-nucleon transfer and knockout processes. S_{2n} are the two-neutron separation energies.

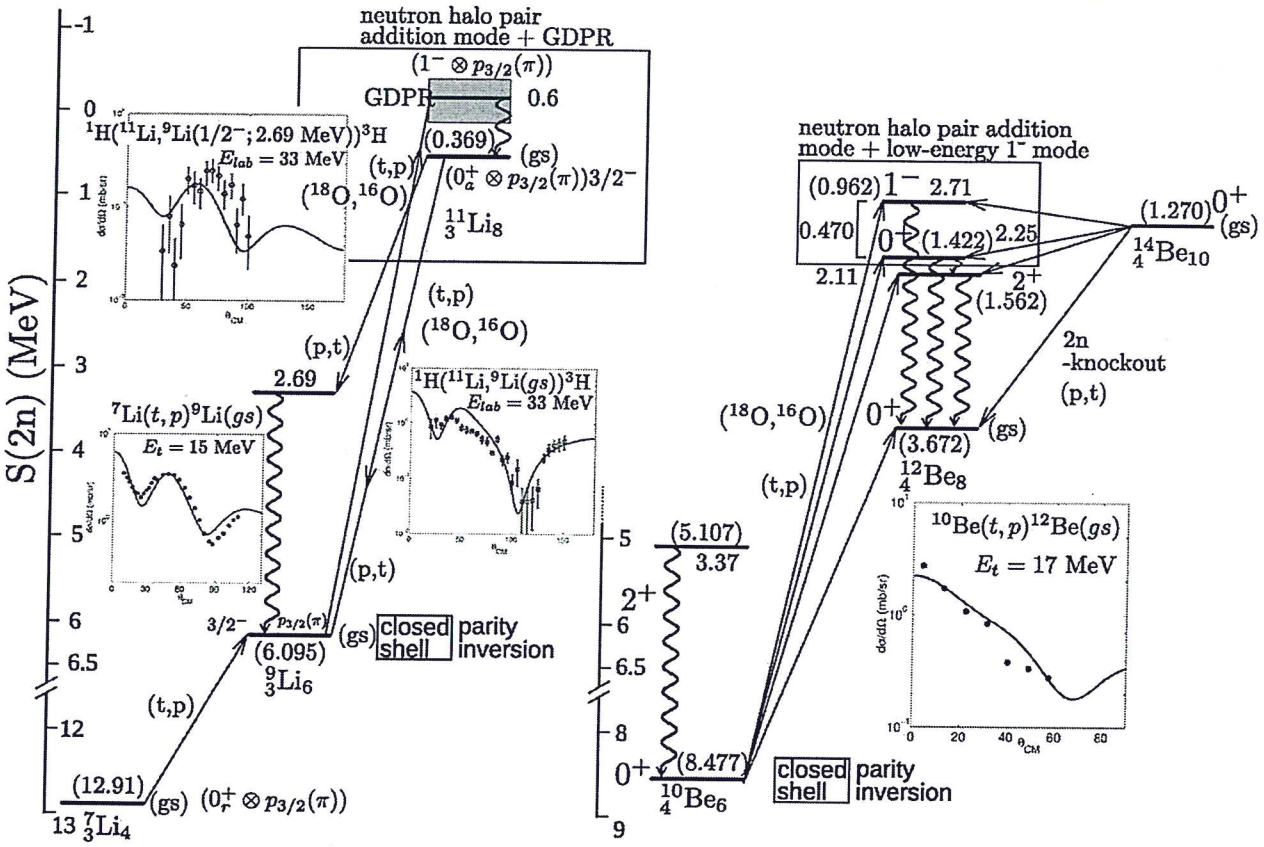

Figure A5. Monopole pairing vibrational modes associated with $N = 6$ parity inverted closed shell isotopes, together with low-energy $E1$-strength modes. The levels are displayed as a function of the two-neutron separation energies $S(2n)$. These quantities are shown in parenthesis on each level, the excitation energies with respect to the ground state are quoted in MeV. In four of the insets, absolute differential cross sections from selected (t, p) and (p, t) reactions calculated as described in the text (see. [90, 164]), are shown in comparison with the experimental data [165, 166].

Which of the two pictures is more adequate to describe the dipole mediated Cooper binding is an open question, as each of them reflects important physical properties which characterize the GDPR. In any case, both indicate the symbiotic character of the halo Cooper pair addition mode and of the pygmy resonance built on top of, and almost degenerate with it. Insight into this question can be obtained by shedding light on the question of whether the velocity field of each of the symbiotic states is more similar to that associated with irrotational or vortex-like flow[32] (~~within this context see [161]~~). ~~Some insight into this question~~ see Repko et al (2013) One ~~could be shed through electron scattering experiments, likely not an easy task when dealing with unstable nuclei. On the other hand,~~ two-nucleon transfer reactions, specific probe of (multipole) pairing vibrational modes, contain many of the answers to the above question (figure A3). In fact, ground state correlations will play a very different role in the absolute value of the ^{9}Li(t, p)^{11}Li (1^-) cross section, depending on which picture is correct. In the case in which it can be viewed as a vortex (pair addition dipole mode) it will lead to an increase of the two-particle transfer reaction (positive coherence). It will produce the opposite effect if the correct interpretation of the GDPR is that of a (p–h)-like excitation [76]. Insight in the above question may also be obtained by studying the properties of a quantal vortex in a Wigner cell with parameters which approximately reproduce the halo of ^{11}Li. Within this context, and for the solely purpose of providing an analogy, we refer to what is done in the study of vortices in the environment of neutron stars [162, 163]. 6.I.3

A test of the soundness of the physics discussed above, concerns the question of whether the first excited, 0^+ halo state ($E_x = 2.25$ MeV) of ^{12}Be can be viewed as the |gs(^{11}Li)> in a new environment. In other words, to consider the halo neutron pair addition mode a novel mode of elementary excitation: neutron halo pair addition mode of which the $|1^-(^{12}Be)$;

[32] Within this context, ~~one~~ can mention that a consistent description of the GQR and of the GIQR is obtained assuming that the average eccentricity of neutron orbits is equal to the average eccentricity of the proton orbits [65], the scenario of neutron skin. The isoscalar quadrupole-quadrupole interaction is attractive. Furthermore, the valence orbitals of nuclei have, as a rule and aside from intruder states, homogeneous parity. These facts preclude the GQR to play the role of the GQPR. In fact, there will always be a low-lying quadrupole vibration closely connected with the aligned coupling scheme and thus with nuclear plasticity. Within this context one can nonetheless posit that the GQR, related to neutron skin, is closely associated with the aligned coupling scheme. Making a parallel, one can posit that the GDPR is closely connected with vortical motion. Arguably, support for this picture is provided by the low-lying E1 strength of ^{11}Li. It results from the presence of $s_{1/2}$ and $p_{1/2}$ orbitals almost degenerate and at threshold, leading to a low-lying Cooper pair coupled to angular momentum 1^-. (Dipole pair addition mode). The scenario of vortical motion.

(Bes et al 1975)

**) Avogadro et al 2007 and 2008

*) Broglia et al 1971

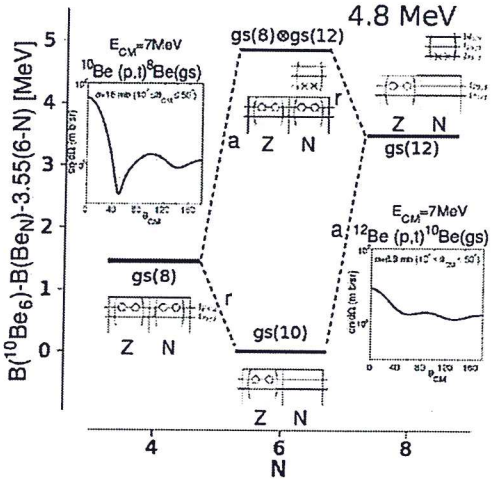

Figure B1. Pairing vibrational spectrum around ^{10}Be and associated absolute two-nucleon transfer differential cross section calculated as explained in the text (reprinted with permission from [164]. Copyright Pleiades Publishing, Ltd. 2014).

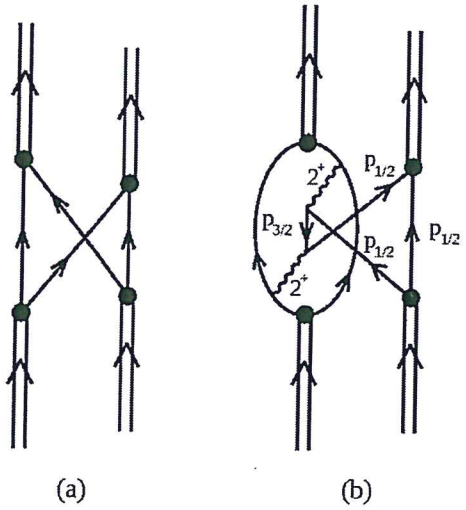

Figure B2. Pairing modes phonon–phonon interaction arizing from: (a) Pauli principle processes between pairing modes, and (b) between single-particle and ph- phonon mediated induced pairing interaction (so called CO diagrams, see e.g. [115]. Reprinted with permission from [164]. Copyright Pleiades Publishing, Ltd. 2014.

2.71 MeV⟩ is a fraction of its symbiotic GDPR partner. One can gain insight concerning this question, by eventually measuring the E1-branching ratio $|1^-$ (2.71 MeV)⟩ → $|0^{+*}$ (2.25 MeV)⟩), and possibly finding other low-energy E1-transitions populating the 0^* state, as well as through two-nucleon stripping process, as well as two-nucleon pickup and knockout reactions (figure A4). A resumé of the picture discussed above is given in figure A5

6.I.4

6.I.5

Appendix B. The pairing vibrational spectrum of ^{10}Be

Calculations similar to the ones discussed in previous sections have been carried out in connection with the expected $N = 6$ shell closure in ^{10}Be (see e.g. [167]). In figure B1 we display the associated pairing vibrational spectrum in the harmonic approximation. Also given are the absolute two-nucleon transfer differential cross sections associated with the excitation of the one-phonon pair addition and pair subtraction modes excited in the reactions ^{12}Be(p, t)^{10}Be(gs) and ^{10}Be(p, t)^{8}Be(gs) respectively, calculated for a bombarding energy appropriate for planned studies making use of inverse kinematic techniques [168].

The ((2p–2h)-like) two-phonon pairing vibration state of ^{10}Be is expected, in this approximation, to lie at 4.8 MeV, equal to the sum of the energies of the pair removal $W_1(\beta = -2) = 0.5$ MeV and of the pair addition $W_1(\beta = 2) = 4.3$ MeV modes. In keeping with the fact that the lowest known 0^+ excited state of ^{10}Be appears at about 6 MeV [169], we have used this excitation energy in the calculation of the Q-value associated with the ^{12}Be(p, t)^{10}Be (pv) cross section. The associated shift in energy from the harmonic value of 4.8 MeV can, arguably, be connected with anharmonicities of the ^{10}Be pairing vibrational spectrum, (see figures B2 and B3) [43]. Medium polarization effects (see

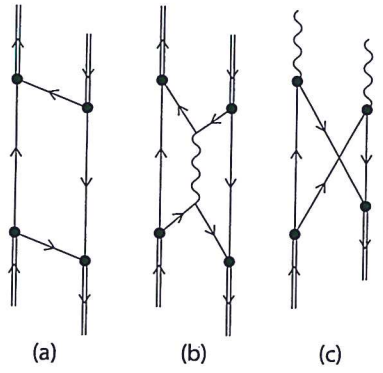

Figure B3. (a) and (b) Examples of pair addition and pair removal modes interactions. (c) Interaction between the two-phonon pairing vibration state and the two-phonon particle-hole state (Reprinted with permission from [164]. Pleiades Publishing, Ltd.).

e.g. figures B2(b) and B3(b)) may also lead to conspicuous anharmonicities in the pairing vibrational spectrum.

The two-nucleon spectroscopic amplitudes corresponding to the reaction ^{10}Be(p, t)^{8}Be(gs) and displayed in table B1, were obtained solving the RPA coupled equations (determinant) associated with the ^{10}Be(gs) pair-removal mode, making use of two pairing coupling constants, to properly deal with the difference in matrix elements (overlaps) between core–core, core–halo and halo–halo two-particle configurations (for details see [164]). In other words with a 'selfconsistent' treatment of the halo particle states ($\varepsilon_k > \varepsilon_F$), in particular of the $d^2_{5/2}(0)$ halo state. The absolute differential cross sections displayed in figure B1 were calculated making use of the optical parameters of [166, 170] and of COOPER [89].